Journal of Biomedical Optics

BiomedicalOptics.SPIEDigitalLibrary.org

# Differentiating intratumoral melanocytes from Langerhans cells in nonmelanocytic pigmented skin tumors *in vivo* by label-free third-harmonic generation microscopy

Wei-Hung Weng
Yi-Hua Liao
Ming-Rung Tsai
Ming-Liang Wei
Hsin-Yi Huang
Chi-Kuang Sun

Wei-Hung Weng, Yi-Hua Liao, Ming-Rung Tsai, Ming-Liang Wei, Hsin-Yi Huang, Chi-Kuang Sun, "Differentiating intratumoral melanocytes from Langerhans cells in nonmelanocytic pigmented skin tumors *in vivo* by label-free third-harmonic generation microscopy," *J. Biomed. Opt.* **21**(7), 076009 (2016), doi: 10.1117/1.JBO.21.7.076009.

# Differentiating intratumoral melanocytes from Langerhans cells in nonmelanocytic pigmented skin tumors *in vivo* by label-free third-harmonic generation microscopy

**Wei-Hung Weng,[a,b] Yi-Hua Liao,[a,c,*] Ming-Rung Tsai,[a] Ming-Liang Wei,[a] Hsin-Yi Huang,[d] and Chi-Kuang Sun[a,e,f,*]**
[a]National Taiwan University, Molecular Imaging Center, No. 1, Section 4, Roosevelt Road, Da'an District, Taipei 10617, Taiwan
[b]Harvard Medical School, Department of Biomedical Informatics, 10 Shattuck Street, Boston, Massachusetts 02115, United States
[c]National Taiwan University Hospital and National Taiwan University College of Medicine, Department of Dermatology, No. 7, Zhongshan S Road, Zhongzheng District, Taipei 100, Taiwan
[d]National Taiwan University Hospital and National Taiwan University College of Medicine, Department of Pathology, No. 7, Zhongshan S Road, Zhongzheng District, Taipei 100, Taiwan
[e]National Taiwan University, Department of Electrical Engineering and Graduate Institute of Photonics and Optoelectronics, No. 1, Section 4, Roosevelt Road, Da'an District, Taipei 10617, Taiwan
[f]Massachusetts Institute of Technology, Research Laboratory of Electronics, 77 Massachusetts Avenue, Cambridge, Massachusetts 02139, United States

**Abstract.** Morphology and distribution of melanocytes are critical imaging information for the diagnosis of melanocytic lesions. However, how to image intratumoral melanocytes noninvasively in pigmented skin tumors is seldom investigated. Third-harmonic generation (THG) is shown to be enhanced by melanin, whereas high accuracy has been demonstrated using THG microscopy for *in vivo* differential diagnosis of nonmelanocytic pigmented skin tumors. It is thus desirable to investigate if label-free THG microscopy was capable to *in vivo* identify intratumoral melanocytes. In this study, histopathological correlations of label-free THG images with the immunohistochemical images stained with human melanoma black (HMB)-45 and cluster of differentiation 1a (CD1a) were made. The correlation results indicated that the intratumoral THG-bright dendritic-cell-like signals were endogenously derived from melanocytes rather than Langerhans cells (LCs). The consistency between THG-bright dendritic-cell-like signals and HMB-45 melanocyte staining showed a kappa coefficient of 0.807, 84.6% sensitivity, and 95% specificity. In contrast, a kappa coefficient of −0.37, 21.7% sensitivity, and 30% specificity were noted between the THG-bright dendritic-cell-like signals and CD1a staining for LCs. Our study indicates the capability of noninvasive label-free THG microscopy to differentiate intratumoral melanocytes from LCs, which is not feasible in previous *in vivo* label-free clinical-imaging modalities.  [DOI: 10.1117/1.JBO.21.7.076009]

Keywords: *in vivo*; virtual biopsy; third-harmonic generation microscopy; label-free; intratumoral melanocytes; Langerhans cells; human melanoma black-45; cluster of differentiation 1a.

Paper 150856RRR received Dec. 21, 2015; accepted for publication Jun. 20, 2016; published online Jul. 18, 2016.

## 1 Introduction

Melanocytes present in the skin and hair follicles play a crucial role in the cutaneous pathophysiology. Melanocytes synthesize melanin in specialized organelles, the melanosomes, and transfer melanosomes to the neighboring keratinocytes through their dendritic processes to protect cells against UV photodamage.[1–3] Melanocyte dendrites are arborizing and branching protoplasmic processes, which function to provide a conduit for melanosome trafficking to keratinocytes. Melanocyte dendrites are composed of actin and microtubules,[3] and are able to respond to various growth factors that stimulate or inhibit dendrite formation. Keratinocyte-derived factors, including endothelin 1 (ET1), nerve growth factor (NGF), $\alpha$-melanocyte-stimulating hormone ($\alpha$-MSH), adrenocorticotrophic hormone, prostaglandin E2 (PGE2), prostaglandin F2$\alpha$ (PGF2$\alpha$), and $\beta$-endophin, have been demonstrated to play a role in melanocyte dendriticity.[4,5] A variety of factors related to cytoskeleton such as integrins,[6] Rho, or Rac proteins also mediate dendrite formation as well.[7] For example, it has been reported that $\alpha$-MSH inhibits Rho by increasing cAMP levels and, therefore, results in enhancing melanocyte dendriticity.[7] As the morphology of melanocyte dendrites are influenced by the biological mediators secreted in the local microenvironment, the characteristics of dendritic processes of intratumoral melanocytes may differ in various pigmented skin tumors.

The histologic examination of the distribution and cellular morphology of melanocytes is an essential step for the diagnosis of benign and malignant melanocytic skin tumors, including melanocytic nevus, dysplastic nevus, and malignant melanoma. For example, atypical melanocytes with pagetoid spread, horizontal, or vertical growth are important diagnostic histopathological criteria for malignant melanoma.[8] The majority of melanocytes reside in the basal epidermis, where melanocytes are surrounded by keratinocytes with an approximate ratio of one melanocyte per five to six keratinocytes, and form epidermal melanin units.[3] It has been demonstrated that melanocytic

*Address all correspondence to: Yi-Hua Liao, E-mail: yihualiao@ntu.edu.tw; Chi-Kuang Sun, E-mail: sun@ntu.edu.tw

proliferation, containing prominent dendrites and copious amounts of cytoplasmic melanin, is associated with or mixed with the original tumor cell growth in a variety of nonmelanocytic skin tumors. The examples include melanoacanthoma, a variant of pigmented seborrheic keratosis (SK), pigmented actinic keratosis, pigmented Bowen's disease, and pigmented squamous cell carcinoma.[9,10] Melanocytes are also present in hair bulbs.[3] Therefore, tumors derived from the follicle appendage including trichoblastoma, basal cell carcinoma (BCC), and rarely pilomatricoma are also encountered to possess hypertrophied dendritic melanocytes.[10] Nonetheless, the intratumoral melanocytes in these nonmelanocytic skin tumors are seldom investigated before.[11,12] As the morphology, distribution, and dendrite formations of intratumoral melanocytes can be influenced by the microenvironment in different skin tumors, the analysis of intratumoral melanocytes will be important in making diagnosis of nonmelanocytic pigmented tumors. Yet, the standard methodology for confirmation of the existence of melanocytes is by human melanoma black (HMB)-45, Melan-A, or S-100 immunohistochemical (IHC) study to detect positive-stained cells with dendritic processes.[8] Nevertheless, time-consuming and labor-intensive procedures including invasive skin biopsy, tissue preparation, section, and immunostaining are inevitable for this traditional approach.

The pursuit to improve bedside clinical diagnosis, while minimizing unnecessary skin biopsies, has led to the development of several *in vivo* skin-imaging techniques. As melanin provides strong contrast for reflectance confocal microscopy (RCM),[12–16] several studies have evaluated the diagnostic accuracy of *in vivo* RCM for differentiation between benign and malignant melanocytic skin tumors.[13–15,17–20] Remarkably, 93% sensitivity and 76% specificity could be reached by RCM, which has a sensitivity superior to the diagnostic accuracy achieved with dermoscopy.[21,22] In addition, *in vivo* multiphoton microscopy was exploited to distinguish melanocytic nevi, dysplastic nevi, and melanoma through the characteristic morphologic features of melanocytes.[23] Intratumoral melanocytes could also be identified in nonmelanocytic tumors such as pigmented BCC by *in vivo* RCM.[11,24,25] However, it is hard to differentiate melanocytes from intraepidermal Langerhans cells (LCs), since both are cells with prominent dendritic processes and share similar morphology under RCM.[11,25,26] Thus an improved *in vivo* imaging modality is needed for making a clear differentiation between melanocytes and LCs.

Harmonic generation microscopy (HGM) has been proved to have high performance on *in vivo* human tissue observation with the characteristics of high resolution, deep penetration, and noninvasiveness.[27–34] Based on the principle of third-order nonlinear processes, the melanin-enhancement nature of label-free third-harmonic generation (THG) in HGM has been confirmed in the previous study.[28] We have also demonstrated that HGM achieved high diagnostic accuracy in nonmelanoma pigmented skin lesions such as BCC, SK, and melanocytic nevus.[33] Taking advantage of HGM and the characteristic of melanin as a strong source of THG contrast, in this work, we demonstrate the unique THG microscopic capability to identify intratumoral melanocytes and to differentiate them from LCs without any external labeling. Through *in vivo* and *ex vivo* THG microscopic imaging and IHC staining with HMB-45 and cluster of differentiation 1a (CD1a) in various kinds of pigmented skin neoplasms including pigmented BCC, SK, and melanocytic nevus, the correlation between THG-bright dendritic-cell-like signals and HMB-45 positivity was established, which indicated the origin of cells with dendritic processes under label-free THG imaging as melanocytes. In addition, we report the capability of THG microscopy to provide different morphological patterns of dendritic cells in different pigmented skin tumors *in vivo*, which makes noninvasive label-free THG microscopy especially useful for their differential diagnosis.

## 2 Materials and Methods

### 2.1 *Subjects*

Seventeen patients aged 34 to 85 years were recruited from the Dermatology Clinic at National Taiwan University Hospital. All the patients were Asians and their skin phototypes were Fitzpatrick type III or IV. THG microscopic images were obtained *in vivo* on 11 patients with pigmented skin tumors before surgical biopsy or excision and were obtained *ex vivo* on 6 surgical specimens. The THG images were acquired from both lesions and surrounding clinical normal counterparts for comparison. All excised specimens were sent to the Department of Pathology for histopathological examination for the final pathological diagnosis. There were four melanocytic nevi (four *in vivo*), one melanoma (one *ex vivo*), four SK (four *in vivo*), and eight pigmented BCC (five *ex vivo* and three *in vivo*; nodular or superficial type). The image acquisition by THG microscopy was performed under the Institutional Review Board protocol reviewed and approved by the Research Ethics Committee of National Taiwan University Hospital. Informed consent was obtained from each subject before enrollment.

### 2.2 *Third-Harmonic Generation Microscopy*

The dataset of images was acquired from the label-free THG microscopy, which was modified from a commercial scanning system (Olympus, FV300) and was excited by a Cr: forsterite laser with a wavelength of 1230 nm, a pulse width of 100 fs, and a repetition rate of 110 MHz as the previous HGM study.[33] The wavelength of 1230 nm was proved to have minimal light attenuation in human skin tissues.[35] Noninvasiveness evaluation of HGM also demonstrated that excitation light scattering and pigment absorption in the skin was minimized at the wavelength of 1230 nm.[28] Skin or skin samples were excited by the collimated laser beam transmitted through the scanning system, an 865-nm dichroic beam splitter (DBS1), and an infrared water immersion objective (Olympus, UPlanApo/60 × /NA = 1.2). The backward harmonic generation signals were collected by the same objective and reflected by DBS1 to two photomultiplier tubes [Hamamatsu R4220P for THG and Hamamatsu R928P for second harmonic generation (SHG)]. SHG and THG signals were then separated by a 490-nm dichroic beam splitter (DBS2) and were filtered by two bandpass filters (D410/30 for THG and D615/10 for SHG) inserted.

Submicron spatial resolution with lateral resolution less than 0.7 $\mu$m at a 270-$\mu$m depth could be achieved for THG,[33] which was the primary contrast modality for observation of melanocytes in skin tissues. For each image stack, the process of imaging was less than 1 min and the total exposure time of the laser light for each volunteer was less than 30 min. The average excitation power after the objective was around but slightly less than 100 mW. The accumulated photon energy was less than 180 J in each volunteer. Under such an accumulated laser dosage, no erythema, pigmentation, or blister formation on the examined

skin and skin samples were found. In the histopathological examinations, no evidence of photodamage, such as coagulation necrosis, on the illuminated specimens was identified.[27,28,31–34]

### 2.3 *Third-Harmonic Generation Microscopic Features of Melanocytes*

Normal epidermal stratification of the stratum corneum, stratum granulosum, stratum spinosum, and stratum basale can be visualized in serial HGM sections label-free and has already been described before.[27,28,31–34] The irregular THG-bright cells with dark nuclei and multiple cellular processes longer than the cell bodies were found mainly in the basal layer of the epidermis and inside certain tumors through THG microscopic imaging without any staining to the skin tissues. Due to the strong THG signals, enlarged cell volumes, and irregular shapes with several dendritic processes, the dendritic cells can be morphologically distinguished from the surrounding small, polygonal basal keratinocytes (Fig. 1).

### 2.4 *Antibodies and Immunohistochemical Study*

The antibodies used included antihuman HMB-45 (clone HMB45, Agilent Technologies, Dako, Denmark) and anti-CD1a (clone JPM30, LEICA Biosystems, Singapore) antibodies. Immunohistochemistry was performed as previously described.[36] Diaminobenzidine (DAB; Agilent Technologies, Dako, Denmark) was applied for colorization and the slides were counterstained for nuclei with hematoxylin. The sections were examined double blindly by two pathologists.

### 2.5 *Image Analysis and Statistics*

The THG microscopic images of 17 pigmented skin tumors were retrospectively analyzed by two independent pathologists in a blinded fashion (blinded to participant name, sex, age, and diagnosis), since the current gold standard for pathological images is based on vision interpretation. The interpretation was based on the stack imaging reading (three-dimensional reading). The observers were instructed in the interpretation of the en face HGM images using more than 1900 representative HGM images before the assessment and evaluated the interclass correlation coefficients (ICCs) between raters by using the ICC function in psych package of R software.[37,38]

During the assessment, the presence or absence of the THG-bright dendritic-cell-like signals as well as the positivity of IHC staining were documented under observers' general assessment for both the images above the stratum basale (the suprabasal layer) and the images of basal layer/tumor in each individual case. After blinded evaluation of THG and IHC images, the THG microscopic results were compared to the IHC findings that were exploited as the gold standard. Cohen's kappa coefficient test was performed for consistency reliability test. The analysis of sensitivity and specificity was also demonstrated with cross tabulation to understand the diagnostic performance of THG microscopic imaging for melanocytes by using the kappa2 function in irr package of R software.[37,39]

## 3 Results

### 3.1 *Good Level of Inter-Rater Reliability in Analyzing Third-Harmonic Generation Images*

To establish the inter-rater reliability of THG microscopic imaging evaluation between the two observers, the consistency test of the THG microscopic imaging concordance for the epidermis was performed first by examining 1964 THG microscopic images. An ICC value of 0.95 was obtained, which represented an excellent agreement between the two qualified and pretrained physicians. The morphological identification of THG-bright dendritic-cell-like signals was, therefore, performed in 17 cases with pigmented skin tumors and their normal counterparts, with 204 image stacks in total.

### 3.2 *Third-Harmonic Generation Microscopic Imaging Failed to Enhance Langerhans Cells*

LCs are located in the epidermis above the basal layer, mainly in the suprabasal layer including stratum spinosum and stratum granulosum.[11,40] When normal skin tissue was observed from a vertical section by HGM *ex vivo*, we found the THG-bright dendritic cells were located in the stratum basale but not in the suprabasal layers [Fig. 2(a)]. The results implied that LCs were not enhanced under THG microscopy. The commonly used IHC staining for LCs was CD1a or S-100. We did not

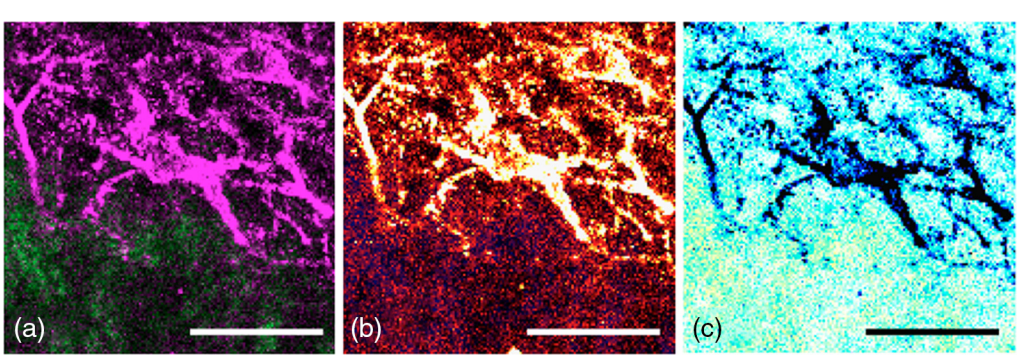


**Fig. 1** THG-bright dendritic-cell-like signals in different color codes. The enlarged, irregular shaped, dendritic-cell-like strong signals were observed in THG channel, and different color codes were applied to assist the identification of THG signals. (a) The magenta/green color code demonstrated THG signals in magenta and SHG in green. (b) The autumn color code of Olympus FluoView application software enhanced the THG signals but also emphasized the background noise. SHG was not shown. (c) The inverse of autumn color code reduced the background noise and made the image similar to traditional histological slides. Yet it decreased the contrast of THG signals. The magenta/green color code was chosen for further analysis. The THG image was acquired *ex vivo*. Bars = 50 $\mu$m.

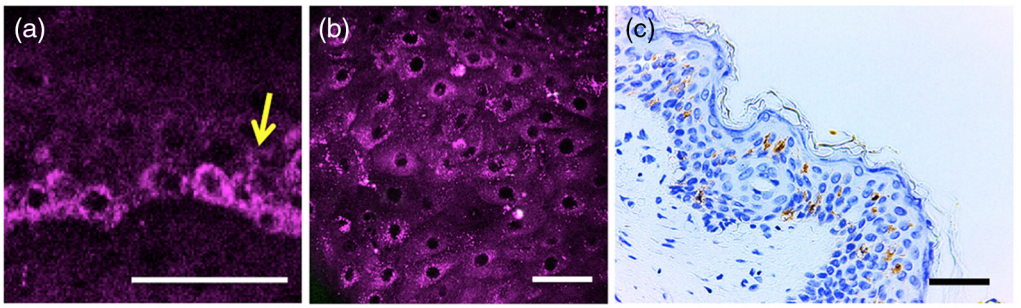


**Fig. 2** CD1a-positive LCs in the suprabasal epidermis could not be enhanced by THG. (a) Vertical view of normal human skin by HGM showed THG-bright dendritic cells (arrow) were limitedly distributed in the basal layer. The representative samples (b) and (c) of the normal epidermis were used to make a correlation between THG microscopic images and CD1a IHC study that stained positively for LCs. (b) The HGM images showed negative results for THG-bright dendritic-cell-like signals in the stratum spinosum, yet (c) CD1a stained positively for suprabasal dendritic cells. The THG images were acquired *ex vivo*. Bars = 50 $\mu$m.

use S-100 immunostaining for LC identification in this study, because the melanocytes were concomitantly stained. To investigate if LCs can be enhanced in THG microscopic images, the blinded evaluation of THG images was compared to the record of THG images acquisition for lesions or normal counterparts and, also, compared to the final pathological judgment for diagnosis. For those images acquired from nontumor suprabasal layer in the 17 cases, the THG images evaluation by physicians were correlated with CD1a immunostaining. Most of the cases revealed negative findings of THG-bright dendritic-cell-like

**Table 1** The suprabasal or basal/tumor distribution of THG-bright dendritic-cell-like signals and HMB-45- or CD1a-positive cells in 17 recruited pigmented skin tumors.

| | | | | | | THG | | HMB-45 | | CD1a | |
|---|---|---|---|---|---|---|---|---|---|---|---|
| Case no. | Sampling | Age | Gender | Location | Pathological diagnosis | Suprabasal | Basal/tumor | Suprabasal | Basal/tumor | Suprabasal | Basal/tumor |
| 1 | *ex vivo* | 73 | M | Left postauricular | BCC, nodular | + | + | + | + | + | — |
| 2 | *ex vivo* | 85 | M | Left postauricular | BCC, nodular | — | + | — | + | + | + |
| 3 | *ex vivo* | 64 | M | Left medial canthus | BCC, nodular | — | + | — | + | + | — |
| 4 | *ex vivo* | 66 | M | Left postauricular | BCC, nodular | — | + | — | + | + | — |
| 5 | *ex vivo* | 70 | F | Nose | BCC, superficial | — | + | — | + | + | — |
| 6 | *in vivo* | 49 | F | Nose | BCC, infiltrative | + | + | — | + | + | — |
| 7 | *in vivo* | 82 | F | Right nasal ala | BCC, nodular | — | + | — | + | + | — |
| 8 | *in vivo* | 64 | M | Right lower cheek | BCC, nodular | — | + | — | + | + | + |
| 9 | *ex vivo* | 63 | M | Right flank | Malignant melanoma, superficial spreading | + | + | + | + | + | — |
| 10 | *in vivo* | 34 | F | Right forearm | Compound nevus | — | — | — | + | + | + |
| 12 | *in vivo* | 39 | F | Abdomen | IDN | — | NA | — | + | + | — |
| 13 | *in vivo* | 57 | F | Left temporal scalp | IDN | — | — | — | — | + | — |
| 14 | *in vivo* | 64 | F | Right abdomen | SK | — | — | — | — | + | + |
| 15 | *in vivo* | 39 | M | Left temporal scalp | SK | — | — | — | — | + | + |
| 16 | *in vivo* | 77 | M | Left preauricular | SK | — | — | — | — | + | + |
| 17 | *in vivo* | 57 | F | Back | SK | — | — | — | — | + | — |

Note: BCC, basal cell carcinoma; SK, seborrheic keratosis; IDN, intradermal nevus; NA, not applicable.

**Table 2** Correlation of THG-bright dendritic-cell-like signals with HMB-45 or CD1a immunohistochemical staining, respectively.

| | Kappa | Sensitivity (%) | Specificity (%) | Accuracy (%) | PPV (%) | NPV (%) |
|---|---|---|---|---|---|---|
| THG versus HMB-45 | 0.807 | 84.6 | 95 | 90.9 | 91.7 | 90.5 |
| THG versus CD1a | −0.37 | 21.7 | 30 | 24.2 | 41.7 | 14.3 |

Note: Kappa, kappa coefficient; PPV, positive predicted value; NPV, negative predicted value.

signals in the suprabasal layer under THG microscopy [Fig. 2(b)]. Only few THG-bright dendritic-cell-like signals were presented in the stratum spinosum under THG microscopy in three of 17 cases (17.65%; Table 1). However, the IHC results revealed CD1a-positive dendritic cells in the suprabasal layer in all the cases [17 of 17 cases; Fig. 2(c)]. The results of both suprabasal and basal/tumor layer (33 observations in total) were pooled together to identify the relationship between CD1a staining and THG-bright dendritic-cell-like signals. There were five true-positive, three true-negative, seven false-positive, and 18 false-negative observations. The kappa coefficient between CD1a staining and THG-bright dendritic-cell-like signals under HGM was −0.37, which represented poor agreement between the two evaluation methods. The sensitivity was 21.7%, the specificity was 30%, and the total accuracy was 24.2% (Table 2).

Wilborn et al.[41] have demonstrated that a large number of LCs was localized in the SK. In this study, four cases of SK were selected and examined by CD1a staining and THG microscopy. The results showed that three of four SK cases were positive with CD1a in the tumor, but no cases revealed dendritic-cell-like signals in the tumor under THG microscopy [Figs. 3(a) and 3(b); Table 1]. The HMB-45 immunostaining was also negative [Fig. 3(c)]. Thus, LCs did not show THG-bright signals. We concluded that the THG-bright dendritic-cell-like signals in THG microscopic images were not originated from LCs.

### 3.3 *Intratumoral Melanocytes were Enhanced Under Third-Harmonic Generation Microscopy*

Melanocytes are located in the basal layer of epidermis and also are colonized or entrapped in the tumor nests of pigmented skin neoplasms.[40,42] As our previous study has demonstrated that melanin possesses a strong contrast under THG,[28] the evaluation of THG microscopic images in 17 cases, which were acquired from tumors, were compared with HMB-45 immunostaining for confirming the correlation between the intratumoral melanocytes and the THG-bright dendritic-cell-like signals. The IHC results showed that 12 of 17 cases presented HMB-45 positive dendritic cells in the tumor [Figs. 4(b), 4(d), and 4(f)], while the THG microscopic images showed that 9 of 16 cases (one case was not applicable) presented THG-bright dendritic-cell-like signals in the tumor [Figs. 4(a), 4(c), and 4(e); Table 1]. Thirty-three observations in both suprabasal and basal/tumor layers were pooled to generally evaluate the correlation between HMB-45 staining and THG-bright dendritic-cell-like signals. There were 11 true-positive, 19 true-negative, one false-positive, and two false-negative observations. The kappa coefficient between positive HMB-45 staining and THG-bright dendritic-cell-like signals in THG microscopic images was 0.807, which represented excellent agreement between the two image modalities. There were 84.6% sensitivity, 95.0% specificity, and 90.9% total accuracy between HMB-45 staining and unstained THG microscopic images (Table 2). Hence, the THG-bright dendritic-cell-like signals in THG microscopic images taken from skin tumors corresponded excellently to intratumoral melanocytes, rather than LCs.

### 3.4 *Intratumoral Melanocytes in Basal Cell Carcinoma*

It has been demonstrated that BCCs were populated by both benign melanocytes and LCs.[42,43] Florell et al.[42] have shown by IHC study that benign melanocytes (9/10 cases) and LCs (9/10 cases) were regularly found in BCCs. RCM also revealed that BCC tumor parenchyma were associated with bright dendritic structures, which were identified histologically as either melanocytes or LCs.[11,26] Our previous study also demonstrated that the dendritic-cell-like signals were presented in BCC nests by THG microscopy, without knowing whether these signals

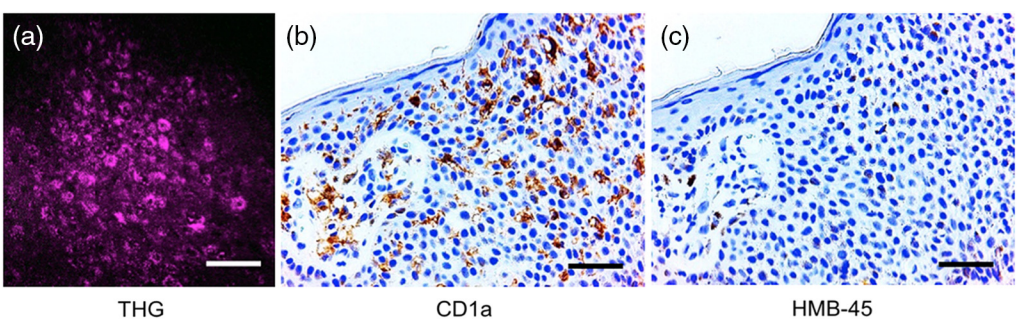


**Fig. 3** Representative *in vivo* label-free THG microscopic and IHC staining images of SK. (a) In the representative case of SK, no THG-bright dendritic-cell-like signals were observed in the tumor. (b) However, CD1a IHC staining, which represented LCs, showed strong-positive immunoreactivity in the tumor site and suprabasal epidermis. (c) HMB-45 staining revealed negative immunoreactivity instead. Bars = 50 $\mu$m.

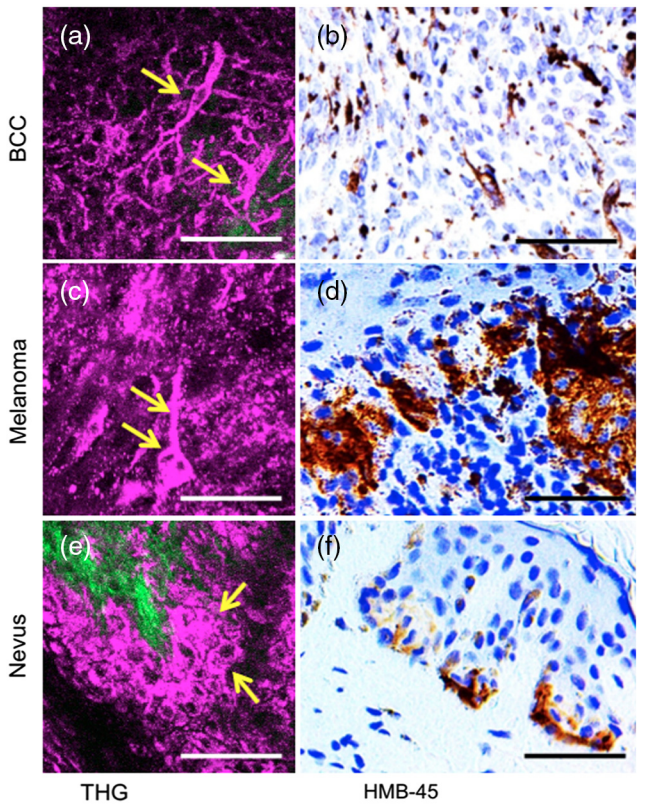


**Fig. 4** Representative label-free THG microscopic images and IHC staining results of BCC, melanoma, and melanocytic nevus. (a) The THG-bright, spindle-shaped, dendritic-cell-like signals (yellow arrows), which represented intratumoral melanocytes, were observed within the tumor of BCC. It had prominent dendrite formation. The cellular processes were slender and longer than those of normal melanocytes. (b) HMB-45 IHC staining also revealed positive staining in the tumor of BCC. (c) In superficial spread malignant melanoma, many large, THG-bright tumor cells with cell size and nuclear polymorphism disrupted the stratification and polarity of the stratum spinosum and basale were noted (yellow arrows). In contrast to the intratumoral dendritic cells in BCC, the cellular processes were wider but shorter in scale than those in BCC. (d) HMB-45 revealed strongly positive staining in melanoma. (e) An increased number of THG-bright dendritic-cell-like signals were scattered in the nevus nests located the basal layer on the elongated rete ridges (yellow arrows). (f) HMB-45 staining showed positive nevus nests along the dermoepidermal junction. The THG images (a) and (b) were acquired *ex vivo* and (c) *in vivo*. Bars = 50 $\mu$m.

were originated from melanocytes or LCs.[33] In this study, the evaluation of intratumoral THG-bright dendritic-cell-like signals in eight pathologically confirmed BCC cases were selected after blinded evaluation and compared with HMB-45 and CD1a IHC analysis. All eight cases of BCC demonstrated positive THG-bright dendritic-cell-like signals in their tumor nests [Fig. 5(a); Table 1]. In IHC study, only two cases of BCC showed positive CD1a staining [25%; Fig. 5(b)] and all eight BCC tumors revealed positive HMB-45 staining [100%; Fig. 5(c)]. Thus, the THG-bright dendritic-cell-like signals in BCC should be concluded as intratumoral melanocytes, in agreement with the conclusion of Sec. 3.3.

### 3.5 *Morphology of Intratumoral Melanocytes in Different Pigmented Tumors Under Third-Harmonic Generation Microscopy*

In the normal epidermis, the dominant THG-bright signals are mainly rounded, regular-shaped basal cells. In BCC, there were many THG-bright dendritic-cell-like signals with elongated or plump cell bodies and long slender cellular processes with complex branching diffusely distributed in the tumor islands [Figs. 4(a) and 5(a)]. In malignant melanoma, the THG-bright dendritic-cell-like signals became large, irregular shaped with atypically bulky and shorter processes compared to those in BCC [Fig. 4(c)]. The melanocytes in benign melanocytic nevi were similar to those in the normal epidermis morphologically [Fig. 4(e)]. The THG microscopy, therefore, demonstrated different morphological patterns of melanocytic dendritic cells in various skin tumors.

## 4 Discussion

Qualitative study is necessary for an image modality like THG microscopy, since the current gold standard is based on the morphological features confirmed by the judgment of dermatopathologists and the results will be able to convert into the foundation of digital imaging processing in the future. Following our previous work,[33] this study first successfully demonstrated the high consistency between THG-bright dendritic-cell-like signals in *in vivo* label-free THG microscopic images and *ex vivo* HMB-45 immunostaining. Since HMB-45 immunostaining is the standard to identify the melanocytes, but not the LCs, we concluded that intratumoral THG-bright dendritic-cell-like signals could represent intratumoral melanocytes while focusing on the BCC cases in this study. This

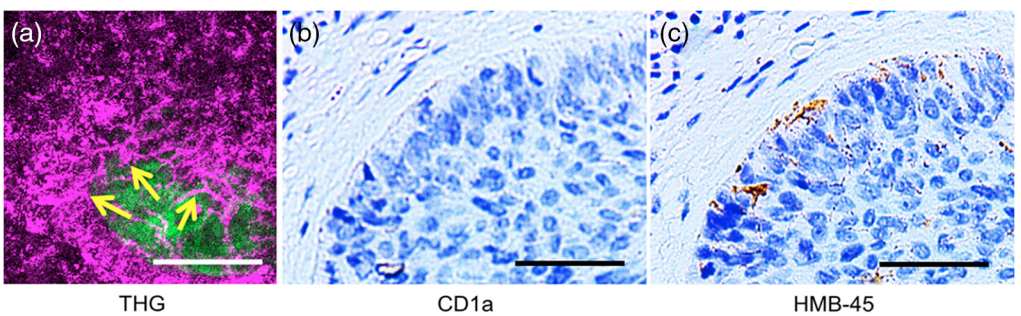


**Fig. 5** *Ex vivo* THG microscopic image and IHC studies of a representative case of BCC. (a) Peripheral palisading cells along the tumor margins could be observed clearly. A large number of THG-bright dendritic-cell-like signals with long and thin cellular processes (yellow arrows) were observed within the tumor nests, which were continuous with the overlying epidermis. (b) IHC studies demonstrated negative CD1a staining in the tumor nests. (c) HMB-45-positive dendritic cells along the tumor border and within the tumor nest, indicating the presence of intratumoral melanocytes. Bars = 50 $\mu$m.

finding may contribute to the fact that intratumoral melanocytes in pigmented BCC are stimulated with melanin-rich cytoplasm and dendritic processes.[44] However, it is uncertain that all melanocytes, both intratumoral and nonintratumoral, can reveal THG-bright dendritic-cell-like signals because melanocytes may not be melanin-rich and dendritic due to their immaturity or loss of activity. As THG microscopic imaging preferentially enhanced dendritic components of melanocytes, but not LCs, it could be beneficial to use THG microscopy to differentiate skin tumors with benign or atypical melanocytes.

Although CD1a positivity was present in some of the tumors in our cases, it is reasonable to identify the THG-bright dendritic-cell-like signals as intratumoral melanocytes based on the following reasons. First of all, the normal distribution of LCs and melanocytes are different. LCs are located in the suprabasal regions of the epidermis while melanocytes primarily reside in the stratum basale of epidermis. From our THG images derived from the normal epidermis, the THG-bright dendritic-shaped cells were majorly revealed in the basal layer just above the SHG-enhanced papillary dermis, which corresponded to the location of melanocytes. Next, although there were abundant LCs present in the tumor part of SK as shown by the CD1a IHC study, no dendrite-like structures were detected under THG microscopy for SK lesions. We propose that because of the THG-enhancing characteristics of melanin or melanin-containing melanosomes,[28] dendritic melanocytes or even basal keratinocytes containing transferred melanosomes demonstrate stronger THG signals than Birbeck granule-containing LCs.

Comparing the morphology of dendritic cells shown by the CD1a and HMB-45 IHC studies, which indicated LCs and melanocytes, respectively, one was unable to differentiate LCs from benign melanocytes by the cell size, shape, dendriticity, and branching complexity. A similar condition was encountered under RCM observation. Segura et al.[26] found that dendritic cells within pigmented basal cell tumor nests, which corresponded to melanocytes, and in the overlying epidermis, which represented LCs, were indistinguishable from each other morphologically. Under RCM, dendritic bright cells in a pagetoid pattern (BCPP) could be observed in both benign melanocytic nevi and melanoma.[25] These bright pagetoid cells most frequently were LCs in nevi but melanocytes in melanomas, and there were no reproducible differences in morphology of BCPP between melanocytic nevi and melanomas;[25] although, Gerger et al.[14] showed that dendrite-like structures with a complex branching pattern were frequently seen in melanoma and less frequently in benign nevi. In comparison to our study, the THG-enhanced dendritic-cell-like signals were specifically recognized as melanocytes, yet the dendritic BCPP shown by RCM could be melanocytes or LCs.[25] Therefore, THG microscopy may have a significant role to increase diagnostic specificity of BCPP for melanoma diagnosis.

We demonstrated in this study that morphological characteristics of intratumoral melanocytes were distinct in different pigmented skin tumors. The morphology of dendritic melanocytes in melanocytic nevus was similar to that in the normal epidermis. Melanoma composed of malignant melanocytic proliferation showed irregularly enlarged atypical THG-bright cells with blunt dendrites. In contrast, the dendritic processes of intratumoral melanocytes scattered between BCC tumor cells were much longer than those in other tumors such as melanoma or benign melanocytic nevi. Although it has been demonstrated that BCC was positive for intratumoral melanocytes, no long dendritic processes were mentioned according to traditional histopathological examination.[42] Segura et al.[26] observed under RCM that long, thin dendritic structures were identified in BCC.[26] However, the etiology of dendritic elongation of intratumoral melanocytes in BCC remains unknown. Previous studies indicated that BCC could highly express basic fibroblast growth factor (bFGF),[45] which was one of the growth factors for melanocyte survival.[46] Furthermore, in addition to bFGF, it was found that supernatant from BCC cell line contained significant amount of ET1 and NGF,[47] both of which can enhance dendrite growth of melanocytes.[3,4] Autocrine or paracrine factors may be, therefore, the possible inducers for long dendritic processes and higher density of intratumoral melanocytes in BCC.

This study has the strengths that we have used the *in vivo* samples to demonstrate the capability of THG *in vivo* imaging. We also evaluated the THG signals morphologically by qualified pathologists and performed statistical analysis, instead of using few selected samples, to solidify the experimental results. However, this study also has some limitations. First, the case numbers were relatively small with only the skin of Fitzpatrick phototypes III to IV. Second, without labeling, THG microscopic imaging could provide easier contrast on active melanocytes with prominent dendritic branching processes than resting melanocytes without obvious dendritic processes since THG microscopic imaging needed to differentiate them from surrounding basal keratinocytes. The cytoplasm of basal cells also revealed strong THG contrasts due to the resonance enhancement of melanin.[28] The strong THG contrast effect also occurred in the stratum corneum because of the multilayer structures of the stratum corneum and lipids within the corneocytes. The same issue was also raised in RCM imaging.[12,48] Finally, it is not feasible to validate the results by colocalization study between THG images and IHC stains. While performing THG imaging on the stained IHC sections, the dye enhancement will yield a perfect but false correspondence. We have worked on a correspondence test between THG-bright dendritic-cell-like signals and cells on unstained histopathological slides, but the comparison was not effective. To capture the THG-bright dendritic-cell-like signals and compare the signals to the cells in the nearest section in the unstained histopathological slide, the section for THG imaging thinner than the average scale of melanocytes (7 to 10 $\mu$m) is necessary. Yet THG imaging of the thinner tissue section will be strongly interfered by the glass surface of slides and coverslips, and results in poor image quality and image distortion because of glass contribution. Thus, the exact correspondence test may not be an available method for validation. However, based on our result of 90.9% total accuracy between HMB-45 staining and unstained THG microscopic images as shown in Table 2, we do not expect to observe a 100% point-to-point correspondence if the colocalization test is feasible.

THG imaging is regarded as a general imaging modality with a high sensitivity to optical inhomogeneity. The conclusion that THG microscopy is with a low sensitivity to the dendrites of intraepidermal LCs seems odd. However, our conclusion is in excellent agreement with a few previous attempts to try to image the intraepidermal LCs *in vivo* with THG microscopy either in human skin or in a murine model of atopic dermatitis.[49,50] Due to the incapability to assess the LCs with THG microscopy, Alexa Fluor 647 and Alexa Fluor 700 were used to stain the LCs for simultaneous two-photon imaging with THG microscopy.[50] We

attribute this conclusion to the following two factors. First, there is limited optical-nonlinear-property inhomogeneity between the dendrites of LCs and their surroundings. Unlike the dendrites of melanocytes, there is no melanin in LCs so that it lacks a major contrast to provide the required nonlinear property inhomogeneity between the dendrites of LCs and their surrounding cells. In our examined images, the enhancement by melanin to the THG intensity can be up to 5 to 10 times, whereas we found that the "brightness" required to be identifiable by a pathologist should be at least 30% higher than the surrounding THG signals. As a result, the second factor to lead to the low sensitivity of LCs is the limited dynamic range of the detection system as well as the digital image. In order not to saturate the THG image with a strong melanin enhancement, as can be seen by comparing Fig. 2(a) with Fig. 2(c), the THG signals from dendrites of LCs will be with an intensity in the order of or lower than the noise background of the clinical system.

In summary, this study indicated the capability of *in vivo* noninvasive THG microscopy to characterize intratumoral melanocytes, which were not identified specifically in previous *in vivo* studies without staining. The high sensitivity of THG microscopy in detecting intratumoral melanocytes is useful as add-on information for improving the accuracy of diagnosis for the pigmented skin tumors such as pigmented BCC, SK, melanocytic nevus, or malignant melanoma while combining the previous HGM diagnostic criteria of these cutaneous lesions.[33] The current human-interpreted morphological study is necessary for THG microscopy to be a potential assistance for pathologists' image reading. Further direction of the THG imaging study will be THG image processing and quantitative analysis of THG signals for automatic feature annotation, pattern identification, and larger-scale image analysis in the future.

## Acknowledgments

This project was supported by grants from the National Health Research Institute (NHRI-EX104-9936EI), the Ministry of Science and Technology, Taiwan (MOST 103-2221-E-002-137-MY3), the National Science Council Taiwan (NSC 102-3011-P-002-010), the Molecular Imaging Center, National Taiwan University (MIC-1, 103R891601), and the National Taiwan University Hospital (NTUH 104-S2794).

## References

1. L. C. Harbor and D. R. Bickers, *Photosensitivity Diseases: Principles of Diagnosis and Treatment*, Saunders, Philadelphia, Pennsylvania (1981).
2. M. A. Pathak et al., "Sunlight and melanin pigmentation," in *Photochemical and Photobiological Reviews*, pp. 211–239, Springer, New York (1976).
3. H. Y. Park and M. Yaar, "Biology of melanocytes," in *Fitzpatrick's Dermatology in General Medicine*, L. A. Goldsmith et al., Ed., pp. 765–780, McGraw-Hill Companies Inc., New York (2012).
4. T. Hirobe, "Role of keratinocyte-derived factors involved in regulating the proliferation and differentiation of mammalian epidermal melanocytes," *Pigm. Cell Res.* **18**(1), 2–12 (2005).
5. S. Kauser et al., "Regulation of human epidermal melanocyte biology by β-endorphin," *J. Invest. Dermatol.* **120**(6), 1073–1080 (2003).
6. M. Hara et al., "Role of integrins in melanocyte attachment and dendricity," *J. Cell Sci.* **107**(10), 2739–2748 (1994).
7. G. Scott, "Rac and rho: the story behind melanocyte dendrite formation," *Pigm. Cell Res.* **15**(5), 322–330 (2002).
8. C. Garbe et al., "Diagnosis and treatment of melanoma. European consensus-based interdisciplinary guideline—update 2012," *Eur. J. Cancer* **48**(15), 2375–2390 (2012).
9. P. Papageorgiou, A. Koumarianou, and R. Chu, "Pigmented Bowen's disease," *Br. J. Dermatol.* **138**(3), 515–518 (1998).
10. M. B. Morgan et al., "Pigmented squamous cell carcinoma of the skin: morphologic and immunohistochemical study of five cases," *J. Cutaneous Pathol.* **27**(8), 381–386 (2000).
11. A. L. C. Agero et al., "Reflectance confocal microscopy of pigmented basal cell carcinoma," *J. Am. Acad. Dermatol.* **54**(4), 638–643 (2006).
12. S. González et al., "Confocal microscopy patterns in nonmelanoma skin cancer and clinical applications," *Actas Dermo-Sifiliogr.* **105**(5), 446–458 (2014).
13. K. J. Busam et al., "Detection of clinically amelanotic malignant melanoma and assessment of its margins by in vivo confocal scanning laser microscopy," *Arch. Dermatol.* **137**(7), 923–929 (2001).
14. A. Gerger et al., "Diagnostic applicability of in vivo confocal laser scanning microscopy in melanocytic skin tumors," *J. Invest. Dermatol.* **124**(3), 493–498 (2005).
15. G. Pellacani et al., "In vivo confocal scanning laser microscopy of pigmented Spitz nevi: comparison of in vivo confocal images with dermoscopy and routine histopathology," *J. Am. Acad. Dermatol.* **51**(3), 371–376 (2004).
16. M. Rajadhyaksha et al., "In vivo confocal scanning laser microscopy of human skin: melanin provides strong contrast," *J. Invest. Dermatol.* **104**(6), 946–952 (1995).
17. K. J. Busam et al., "Detection of intraepidermal malignant melanoma in vivo by confocal scanning laser microscopy," *Melanoma Res.* **12**(4), 349–355 (2002).
18. R. G. Langley et al., "Confocal scanning laser microscopy of benign and malignant melanocytic skin lesions in vivo," *J. Am. Acad. Dermatol.* **45**(3), 365–376 (2001).
19. A. Gerger et al., "*In vivo* confocal laser scanning microscopy in the diagnosis of melanocytic skin tumours," *Br. J. Dermatol.* **160**(3), 475–481 (2009).
20. I. Vaišnorienė et al., "Nevomelanocytic atypia detection by in vivo reflectance confocal microscopy," *Medicina* **50**(4), 209–215 (2014).
21. A. D. Stevenson, S. Mickan, and S. Mallett, "Systematic review of diagnostic accuracy of reflectance confocal microscopy for melanoma diagnosis in patients with clinically equivocal skin lesions," *Dermatol. Pract. Concept.* **3**(4), 19–27 (2013).
22. A. Scope and C. Longo, "Recognizing the benefits and pitfalls of reflectance confocal microscopy in melanoma diagnosis," *Dermatol. Pract. Concept.* **4**(3), 67–71 (2014).
23. M. Balu et al., "Distinguishing between benign and malignant melanocytic nevi by in vivo multiphoton microscopy," *Cancer Res.* **74**(10), 2688–2697 (2014).
24. K. Sauermann et al., "Investigation of basal cell carcionoma by confocal laser scanning microscopy in vivo," *Skin Res. Technol.* **8**(3), 141–147 (2002).
25. P. Hashemi et al., "Langerhans cells and melanocytes share similar morphologic features under in vivo reflectance confocal microscopy: a challenge for melanoma diagnosis," *J. Am. Acad. Dermatol.* **66**(3), 452–462 (2012).
26. S. Segura et al., "Dendritic cells in pigmented basal cell carcinoma: a relevant finding by reflectance-mode confocal microscopy," *Arch. Dermatol.* **143**(7), 883–886 (2007).
27. S. Y. Chen, H. Y. Wu, and C. K. Sun, "In vivo harmonic generation biopsy of human skin," *J. Biomed. Opt.* **14**(6), 060505 (2009).
28. S. Y. Chen et al., "In vivo virtual biopsy of human skin by using noninvasive higher harmonic generation microscopy," *IEEE J. Sel. Top. Quantum Electron.* **16**(3), 478–492 (2010).
29. M. R. Tsai et al., "In vivo optical virtual biopsy of human oral mucosa with harmonic generation microscopy," *Biomed. Opt. Express* **2**(8), 2317–2328 (2011).
30. M. R. Tsai et al., "Characterization of oral squamous cell carcinoma based on higher-harmonic generation microscopy," *J. Biophotonics* **5**(5–6), 415–424 (2012).
31. Y. H. Liao et al., "Determination of chronological aging parameters in epidermal keratinocytes by in vivo harmonic generation microscopy," *Biomed. Opt. Express* **4**(1), 77–88 (2013).
32. M. R. Tsai et al., "Applying tattoo dye as a third-harmonic generation contrast agent for in vivo optical virtual biopsy of human skin," *J. Biomed. Opt.* **18**(2), 026012 (2013).

33. M. R. Tsai et al., "Differential diagnosis of nonmelanoma pigmented skin lesions based on harmonic generation microscopy," *J. Biomed. Opt.* **19**(3), 036001 (2014).
34. Y. H. Liao et al., "Quantitative analysis of intrinsic skin aging in dermal papillae by in vivo harmonic generation microscopy," *Biomed. Opt. Express* **5**(9), 3266–3279 (2014).
35. B. E. Bouma et al., "Self-phase-modulated Kerr-lens mode-locked Cr: forsterite laser source for optical coherence tomography," *Opt. Lett.* **21**(22), 1839–1841 (1996).
36. Y. H. Liao, S. M. Hsu, and P. H. Huang, "ARMS depletion facilitates UV irradiation-induced apoptotic cell death in melanoma," *Cancer Res.* **67**(24), 11547–11556 (2007).
37. R Core Team, "R: a language and environment for statistical computing," R Foundation for Statistical Computing, Vienna, Austria (2015) https://www.R-project.org/ (21 Febraury 2016).
38. W. Revelle, "Psych: procedures for personality and psychological research, R package version 1.5.8," Northwestern University, Evanston, Illinois (2015) http://CRAN.R-project.org/package=psych (21 Febraury 2016).
39. M. Gamer et al., "Irr: various coefficients of interrater reliability and agreement, R package version 0.84." (2012) http://CRAN.R-project.org/package=irr (21 February 2016).
40. R. L. Modlin et al., "Innate and adaptive immunity in the skin," in *Fitzpatrick's Dermatology in General Medicine*, L. A. Goldsmith et al., Eds., pp. 105–125, McGraw-Hill Companies Inc., New York (2012).
41. W. H. Wilborn, D. E. Dismukes, and L. F. Montes, "Ultrastructural identification of Langerhans cells in seborrheic keratosis," *J. Cutaneous Pathol.* **5**(6), 368–372 (1978).
42. S. R. Florell, J. J. Zone, and J. W. Gerwels, "Basal cell carcinomas are populated by melanocytes and Langerhan's cells," *Am. J. Dermatopathol.* **23**(1), 24–28 (2001).
43. B. Schubert and P. Rudolph, "Basal cell carcinoma: a natural milieu for melanocytes?," *Am. J. Dermatopathol.* **23**(6), 558–559 (2001).
44. B. R. Smoller, N. S. McNutt, and A. Hsu, "HMB-45 recognizes stimulated melanocytes," *J. Cutaneous Pathol.* **16**(2), 49–53 (1989).
45. J. L. Arbiser et al., "Altered basic fibroblast growth factor expression in common epidermal neoplasms: examination with in situ hybridization and immunohistochemistry," *J. Am. Acad. Dermatol.* **42**(6), 973–977 (2000).
46. R. Halaban, S. Ghosh, and A. Baird, "bFGF is the putative natural growth factor for human melanocytes," *In Vitro Cell. Dev. Biol.* **23**(1), 47–52 (1987).
47. C. C. E. Lan et al., "Pigmentation in basal cell carcinoma involves enhanced endothelin-1 expression," *Exp. Dermatol.* **14**(7), 528–534 (2005).
48. P. Calzavara-Pinton et al., "Reflectance confocal microscopy for in vivo skin imaging," *Photochem. Photobiol.* **84**(6), 1421–1430 (2008).
49. J.-H. Lee et al., "Noninvasive in vitro and in vivo assessment of epidermal hyperkeratosis and dermal fibrosis in atopic dermatitis," *J. Biomed. Opt.* **14**(1), 014008 (2009).
50. J.-H. Lee et al., "Evaluation of the role of CD207 on Langerhans cells in a murine model of atopic dermatitis by in situ imaging using Cr: forsterite laser-based multi-modality nonlinear microscopy," *J. Biomed. Opt.* **17**(11), 116007 (2012).



**Wei-Hung Weng** received his MD degree from Chang Gung University, Taoyuan, Taiwan, in 2011, and is currently working toward his MMSc degree in biomedical informatics at Harvard Medical School, Boston, MA, USA. His research interests include medical image analysis and applying machine learning and natural language-processing methods to unstructured clinical data.

**Yi-Hua Liao** received her MD degree from the College of Medicine, National Taiwan University, and her PhD from the Graduate Institute of Pathology, College of Medicine, National Taiwan University, Taipei, Taiwan, in 1996 and 2007, respectively. She is now an associate professor in the Department of Dermatology, National Taiwan University, and a supervisor of the Taiwanese Dermatological Association. She is responsible for dermatologic surgery special clinic, cosmetic surgery and laser special clinic.

**Ming-Rung Tsai** received her BS and MS degrees from the National Chiao Tung University, Hsinchu City, Taiwan, and her PhD from the National Taiwan University, Taipei, Taiwan. She works on studying the clinical application of HGM for oral and skin cancer.

**Ming-Liang Wei** received his BS and MS degrees from the National Taiwan University (NTU), Taipei, Taiwan. Currently, he serves as a research assistant at the NTU Molecular Imaging Center and works on studying the clinical application of HGM for skin cancer.

**Hsin-Yi Huang** received her MD degree from the College of Medicine, National Taiwan University, and her PhD from the Graduate Institute of Pathology, College of Medicine, National Taiwan University, Taipei, Taiwan, in 1996 and 2013, respectively. She is now a visiting staff in the Department of Pathology, National Taiwan University Hospital. Her research focuses on neurodegenerative disorders, brain tumors and their biomarkers, as well as pancreatic cancer and its tumorigenesis.

**Chi-Kuang Sun** received his PhD in applied physics from Harvard University in 1995 and was an assistant researcher in the UCSB QUEST Center from 1995 to 1996. In 1996, he joined National Taiwan University, where he is now a distinguished professor of photonics and optoelectronics. He founded the NTU Molecular Imaging Center. His research focuses on nano-acoustics, femtosecond optics, THz optoelectronics, and biomedical imaging. He is a fellow of OSA, SPIE, and IEEE.